

the inelastic channels open at 6.33 MeV; therefore small changes in the position of the resonances have a large impact on the widths. The total 1^- cross section calculated with the present method compares very well with the results of Ref. 2 (cf. Fig. 1). Even the interference pattern at 4.5 MeV is reproduced. The comparison of energies above 6.33 MeV is meaningless because the inelastic channels were neglected in Ref. 2.

7. COMPARISON WITH PREVIOUS METHODS

The method proposed in this paper is intended for the study of the dynamics of a nuclear reaction and especially of its resonance structure. Therefore, everything not directly connected to this aim has been included into an effective interaction. We make no attempt to determine this interaction from a more fundamental point of view (like Ref. 13). A phenomenological residual interaction is used in actual calculations. This attitude is close to the one expressed in Ref. 20 on the basis of the work of Ref. 3. The

formulas given in this paper and those of Ref. 9 essentially coincide, if the renormalization contributions to the matrix elements are dropped and if one neglects the slight difference in treating the single-particle resonance. It might be interesting to note that with our choice of the Hilbert space \mathcal{U}_P , the continuum interaction enters linearly into the reduced K matrix (not the S matrix) [cf. Eq. (41)].

Furthermore, the spirit of our work is closest to the one of Ref. 6, because both methods observe criterion (C2). But the use of approximations Eqs. (22) and (25) reduces the numerical effort considerably in the present calculation. We stress that we have found a solution of the scattering problem that is exact within the Hilbert space \mathcal{U}_P .

ACKNOWLEDGMENTS

One of the authors (J.H.) expresses his gratitude to Professor Feshbach and Professor Kerman for a number of discussions. The advice of E. Bartell in programming is highly appreciated.

Scattering of Medium-Energy Alpha Particles. I. Phenomenological Analysis of Elastic Scattering

DAFNE F. JACKSON AND C. G. MORGAN

Department of Physics, University of Surrey, Guildford, England

(Received 10 May 1968)

Several discrete sets of optical potentials which fit the data on the elastic scattering of medium-energy α particles are examined. It is shown that the usual criterion for equivalence of these potentials is valid only if little variation is allowed in the diffuseness parameter, and that a more widely applicable criterion is obtained by considering the magnitudes of the potentials at the strong-absorption radius. It is also shown that, because of the ambiguities in the optical potential for α particles, the half-way radius and the equivalent radius of the potentials are functions of the depth and therefore cannot be regarded as significant nuclear size parameters. The strong-absorption radius, however, is shown to be a very significant size parameter, which can be related not only to the reflection coefficients but also to the optical-model wave function.

1. INTRODUCTION

IN the standard optical-model analysis of the elastic scattering of medium energy α particles from nuclei the size of the nuclear potential is characterized by the parameters of the Saxon-Woods potential which has the form

$$U(r) = -V_0(1+e^x)^{-1} - iW_0(1+e^{x'})^{-1} \quad (1)$$

with

$$x = (r - R_0)/a, \quad x' = (r - R_0')/a'. \quad (2)$$

The half-way radii R_0 and R_0' are typically some 20–30% larger than the corresponding values for medium-energy nucleon scattering.¹ This difference is

interpreted in terms of the size of the α particle, and the half-way radii are sometimes expressed as²

$$R_0 = z_0 A^{1/3} + c,$$

and similarly for R_0' , where the constant c is 1.7–2.2 F and z_0 is 1.17–1.4 F. More usually, the half-way radii are expressed as

$$R_0 = r_0 A^{1/3}, \quad R_0' = r_0' A^{1/3}.$$

An alternative phenomenological description of elastic scattering is obtained through direct parametrization of the phase shifts δ_L or the reflection coefficients $\eta_L = e^{2i\delta_L}$. The size parameter obtained from an analysis of this type is the strong-absorption radius $R_{1/2}$, which

¹ P. E. Hodgson, *The Optical Model of Elastic Scattering* (Clarendon Press, Oxford, 1963).

² G. Igo and R. M. Thaler, *Phys. Rev.* **106**, 126 (1957).

is defined as³

$$kR_{1/2} = n + \{n^2 + L_0(L_0 + 1)\}^{1/2}, \quad (3)$$

where n is the Coulomb parameter and L_0 is the angular momentum for which $\text{Re}(\eta_L) = \frac{1}{2}$; i.e., $R_{1/2}$ is the classical turning point for a particle of orbital angular momentum L_0 . As pointed out by Alster and Conzett,⁴ there is no reason to expect the value of $R_{1/2}$ obtained from a direct phase analysis to be equal to the value of R_0 obtained from an optical-model analysis of the same data and in general it is found that $R_{1/2} > R_0$. A survey of the data over a range of incident energies has given the formula⁵

$$R_{1/2} = 1.446A^{1/3} + 2.29 \text{ F} \quad (4a)$$

and a further survey at 44 MeV has given⁶

$$R_{1/2} = 1.52A^{1/3} + 2.14 \text{ F}, \quad (4b)$$

with individual nuclei showing substantial deviations from this standard formula. Recently, Blair and Fernandez⁷ have shown that it is possible to connect the methods of phase analysis and optical-model analysis by using an optical potential to generate the reflection coefficients and then defining the corresponding strong-absorption radius, which we shall denote by $R_{1/2}^{\text{OM}}$. The results obtained for $R_{1/2}$ and $R_{1/2}^{\text{OM}}$ by Blair and Fernandez differ by less than 1%.

The equivalent radius of the potential is defined as the radius R_{EQ} of the uniform potential which has the same mean square radius. For a Saxon-Woods potential this is given by

$$R_{\text{EQ}}^2 = R_0^2 + (7/3)\pi^2 a^2 \quad (5)$$

and similarly for the imaginary part. The equivalent radius is of interest for comparison with microscopic analyses of elastic scattering in which it is related to the mean square radius of the nuclear density.⁸ Such an analysis of elastic α -particle scattering has been carried out for the calcium isotopes and will be reported in a subsequent publication.⁹

It is known that there are ambiguities in the optical potentials for strongly absorbed projectiles. Igo¹⁰ has suggested that the depth and shape parameters of the potential can be varied provided that the magnitude

of the potential in the surface region is unchanged, i.e.,

$$V_0 e^{(R_0 - r)/a} = \text{constant}, \quad r > R_0 \quad (6)$$

and similarly for the imaginary part. This criterion is normally reduced to

$$V_0 e^{R_0/a} = \text{constant}, \quad (7)$$

which is a valid statement of Igo's criterion only if the diffuseness parameter a is varied very little. It is also known that the magnitude of the potential in the interior is not irrelevant because it influences the low partial waves which are reflected in the interior of the nucleus,^{11,12} and that several discrete values of V_0 and W_0 can be found which give the same phase shifts for the important partial waves.¹² Drisko *et al.*¹² have shown that these two ambiguities are compatible, although at 43 MeV Igo's condition did not appear to apply to the imaginary part of the potential.

In this paper we examine several discrete sets of optical potentials which fit the data on the elastic scattering of medium energy α particles from various nuclei, and attempt to answer the following questions. (1) Is the Igo criterion for the equivalence of different optical-model potentials valid, either exactly or approximately? (2) Are any other criteria applicable? (3) What size parameters can be extracted from optical-model analyses and what is their physical significance?

2. DISCUSSION OF EXISTING RESULTS

In Table I we list the parameters of sets of optical potentials given in the literature for ⁵⁸Ni,¹³ ¹⁴⁰Ce,¹⁴ and ²⁰⁸Pb,¹⁵ and obtained from analyses of elastic scattering data in the energy region 42–44 MeV. Within each set the values of χ^2 are roughly constant and the size parameters of the imaginary potential are taken to be the same as those of the real part. We note that for ⁵⁸Ni the variation in the diffuseness parameter a is about 1%, and the value of $V_0 e^{R_0/a}$ is roughly constant for the group of potentials. The value of $W_0 e^{R_0/a}$ is not constant, and this is in agreement with the observations of Drisko *et al.*,¹² who also studied ⁵⁸Ni. For ¹⁴⁰Ce and ²⁰⁸Pb the variation in the diffuseness parameter is about 5% and the values of $V_0 e^{R_0/a}$ are no longer constant.

In an optical-model analysis of α particle scattering from ⁵⁸Ni and ²⁴Mg at 24.7 MeV, McFadden and Satchler¹⁶ found very substantial variations in the values of $V_0 e^{R_0/a}$ and $W_0 e^{R_0/a}$, but in these cases the variation in the diffuseness parameter was 10%.

³ J. S. Blair, Phys. Rev. **95**, 1218 (1954); **108**, 827 (1957).

⁴ J. Alster and M. Conzett, Phys. Rev. **136**, B1024 (1964); **139**, B50 (1965).

⁵ W. E. Frahn and R. H. Venter, Ann. Phys. (N. Y.) **24**, 243 (1963).

⁶ J. C. Faivre, H. Krivine, and A. M. Papiou, Nucl. Phys. Phys. **A108**, 508 (1968).

⁷ J. S. Blair and B. Fernandez, University of Washington Report, 1967 (unpublished); and (to be published).

⁸ G. W. Greenlees, G. J. Pyle, and Y. C. Tang, Phys. Rev. Letters **17**, 33 (1966); Phys. Rev. **171**, 1115 (1968); D. F. Jackson and V. K. Kumbhavi, Rutherford High Energy Laboratory PLA Report, 1967 (unpublished).

⁹ D. F. Jackson and V. K. Kumbhavi (to be published).

¹⁰ G. Igo, Phys. Rev. Letters **1**, 72 (1958); **3**, 308 (1959); Phys. Rev. **115**, 1665 (1957).

¹¹ N. Austern, Ann. Phys. (N. Y.) **15**, 299 (1961).

¹² R. M. Drisko, G. R. Satchler, and R. H. Bassel, Phys. Letters **5**, 347 (1963).

¹³ H. W. Broek, J. L. Yntema, B. Buck, and G. R. Satchler, Nucl. Phys. **64**, 259 (1965); H. W. Broek, T. H. Braid, J. L. Yntema, and B. Zeidman, Phys. Rev. **126**, 1514 (1962).

¹⁴ B. Fernandez, University of Washington Report, 1967 (unpublished).

¹⁵ G. R. Satchler, H. W. Broek, and J. L. Yntema, Phys. Letters **16**, 52 (1965).

¹⁶ L. McFadden and G. R. Satchler, Nucl. Phys. **84**, 117 (1966).

TABLE I. Optical potentials for elastic α -particle scattering at 42–44 MeV.

	V_0 (MeV)	W_0 (MeV)	a (F)	r_0 (F)	R_0 (F)	R_{EQ} (F)	$V_0 e^{R_0/a}$	$W_0 e^{R_0/a}$
^{58}Ni	47.6	13.8	0.549	1.585	6.13	6.68	2.58×10^6	7.50×10^5
	69.3	16.4	0.556	1.501	5.72	6.40	2.37	5.60
	105.1	18.6	0.554	1.445	5.60	6.19	2.59	4.58
^{140}Ce	141.9	21.5	0.549	1.409	5.45	6.05	2.98	4.52
	60.6	18.0	0.583	1.483	7.70	8.20	3.42×10^7	1.02×10^7
	70.0	15.7	0.571	1.479	7.68	8.15	5.04	1.13
	151.0	19.2	0.555	1.404	7.29	7.75	7.60	0.97
^{208}Pb	253.1	32.6	0.555	1.350	7.01	7.50	7.58	1.00
	33.3	17.8	0.629	1.485	8.80	9.30	3.99×10^7	2.14×10^7
	34.0	14.6	0.600	1.500	8.89	9.35	9.43	4.05
	93.9	32.0	0.600	1.400	8.30	8.80	9.68	1.51
	114.3	46.3	0.623	1.362	8.07	8.61	5.05	2.04

TABLE II. Optical potentials for elastic α -particle scattering from ^{42}Ca at 42 MeV. The equivalent radius R_{EQ} is given for the real part of the potential only. The value of χ^2 is based on a 10% error in the experimental points.

	V_0 (MeV)	W_0 (MeV)	a (F)	a' (F)	r_0 (F)	r_0' (F)	R_{EQ} (F)	$V_0 e^{R_0/a}$	$W_0 e^{R_0/a'}$	$R_{1/2}^{OM}$ (F)	$V(R_{1/2}^{OM})$	$W(R_{1/2}^{OM})$	χ^2
1	47.0	16.9	0.602	0.604	1.596	1.591	6.25	4.72×10^5	1.60×10^5	7.323	-2.34	-0.83	8.1
2	118.4	19.8	0.599	0.597	1.438	1.546	5.76	4.98	1.61	7.313	-2.44	-0.74	7.3
3	162.8	20.8	0.593	0.589	1.390	1.540	5.61	5.60	1.85	7.318	-2.44	-0.72	6.3
4	212.3	22.3	0.589	0.586	1.354	1.520	5.48	6.27	1.84	7.327	-2.45	-0.66	6.7
5	30.9	18.4	0.648	0.526	1.663	1.667	6.58	2.30×10^5	11.68×10^5	7.332	-2.58	-0.93	8.4
6	84.2	16.7	0.675	0.569	1.430	1.631	5.93	1.33	3.55	7.324	-2.50	-0.86	6.0
7	138.8	17.5	0.759	0.527	1.257	1.667	5.67	0.44	10.43	7.367	-2.63	-0.84	9.6
8	146.3	13.9	0.788	0.545	1.208	1.721	5.65	0.30	8.13	7.377	-2.55	-1.00	10.0
9	1336.0	160.4	0.603	0.605	1.038	1.191	4.65	5.30×10^5	1.50×10^5	7.367	-2.62	-0.77	14.8

TABLE III. Optical potentials for elastic α -particle scattering from ^{42}Ca and ^{50}Ti at 30.5 MeV.

	V_0 (MeV)	W_0 (MeV)	a (F)	a' (F)	r_0 (F)	r_0' (F)	$V_0 e^{R_0/a}$	$W_0 e^{R_0/a'}$	$R_{1/2}^{OM}$ (F)	$V(R_{1/2}^{OM})$	$W(R_{1/2}^{OM})$	χ^2	
^{42}Ca	1	54.6	16.3	0.599	0.603	1.622	1.700	6.68×10^5	2.94×10^5	7.645	-1.85	-0.87	0.88
$\theta < 68^\circ$	2	208.8	28.7	0.603	0.602	1.391	1.593	6.34	2.84	7.661	-1.91	-0.82	1.80
^{50}Ti	1	61.4	16.7	0.588	0.579	1.546	1.490	9.88×10^5	2.19×10^5	7.747	-1.82	-0.32	5.3
$\theta < 130^\circ$	2	242.7	37.3	0.597	0.593	1.327	1.240	8.74	0.83	7.788	-1.87	-0.16	6.2

TABLE IV. Optical potentials for elastic α -particle scattering from ^{50}Ti at 44 MeV.

	V_0 (MeV)	W_0 (MeV)	a (F)	a' (F)	r_0 (F)	r_0' (F)	$V_0 e^{R_0/a}$	$W_0 e^{R_0/a'}$	$R_{1/2}^{OM}$ (F)	$V(R_{1/2}^{OM})$	$W(R_{1/2}^{OM})$	χ^2
1	47.6	20.4	0.610	0.608	1.584	1.505	6.8×10^5	1.86×10^5	7.605	-2.48	-0.67	2.7
2	90.1	24.7	0.588	0.581	1.500	1.457	10.9	2.54	7.616	-2.51	-0.51	2.9
3	196.4	21.9	0.600	0.600	1.354	1.469	8.0	1.81	7.594	-2.52	-0.56	1.7

From this survey we conclude that the usual method of testing the Igo criterion, i.e., through Eq. (7), is not appropriate unless the variation in the diffuseness parameter is small. When the application of Eq. (7) is appropriate the criterion appears to be approximately

TABLE V. Comparison of results for the strong-absorption radii.

	$E=30.5$ MeV ^a	$E=42-44$ MeV ^a	$E=42$ MeV ^b	Eq. (4a)	Eq. (4b)
^{42}Ca	7.65 ± 0.03	7.35 ± 0.03	7.385	7.32	7.43
^{50}Ti	7.77 ± 0.03	7.61 ± 0.03	7.586	7.62	7.75

^a This work.
^b Reference 7.

satisfied for the real part of the potential but not for the imaginary part.

Examination of the sets of potentials also shows that as the depth V_0 increases, the half-way radius R_0 decreases, and hence the mean square radius and the equivalent radius R_{EQ} are functions of V_0 . The same effect is observed at 24.7 MeV.¹⁶ This means that, because of the ambiguities in the phenomenological potentials for strongly absorbed projectiles, nuclear size information cannot be extracted unambiguously from the equivalent radius. Even comparison of values of R_0 for different nuclei is subject to uncertainty if there are variations in the corresponding values of V_0 .

3. NEW RESULTS FOR ^{42}Ca AND ^{50}Ti

As part of a study¹⁷ of inelastic scattering from ^{42}Ca and ^{50}Ti , we have analyzed the data on elastic scattering from ^{42}Ca at 42 MeV,¹⁸ on ^{42}Ca and ^{50}Ti at 30.5 MeV,¹⁹ and on ^{50}Ti at 44 MeV.²⁰

The first group of potentials for ^{42}Ca at 42 MeV given in Table II were obtained by allowing very little variation in the diffuseness parameters a and a' . For these potentials it can be seen that the Igo criterion is approximately satisfied for both the real and imaginary parts of the potentials. By plotting the reflection coefficients given by these potentials we have determined the strong-absorption radius $R_{1/2}^{\text{OM}}$. We have also calculated the magnitude of the optical potential at the strong-absorption radius and find that the real part is quite remarkably constant.

The second group of potentials given in Table II were obtained by allowing the parameters to vary quite freely. In this case the Igo criterion in the form of Eq. (7) cannot be satisfied because of the large variation in the diffuseness parameters. On the other hand, the real potential at the strong-absorption radius is again quite remarkably constant. The same is true for the very deep potential obtained for ^{42}Ca , which is given in the last line of Table II, for the potentials obtained for ^{42}Ca and ^{50}Ti at 30.5 MeV, some of which are given in Table III, and for the potentials for ^{50}Ti at 44 MeV, which are given in Table IV. We therefore propose that a criterion for the equivalence of optical-model potentials for strongly absorbed projectiles is the requirement that the real parts of the potentials should be equal at the strong-absorption radius. Our results also suggest that the imaginary parts of the potentials at the strong-absorption radius should be small and approximately equal.

In Figs. 1-3 we compare the real and imaginary parts of the reflection coefficients η_L and the absorption coefficients $1 - |\eta_L|^2$ for several of the potentials given in Tables II and III. It can be seen that the real and imaginary parts of η_L are not very smooth functions of L . This effect was noted at 24.7 MeV by McFadden and Satchler,¹⁶ who questioned the accuracy of smooth parametrizations of η_L as functions of L . In contrast, from our results it appears that the function $1 - |\eta_L|^2$ shows much smoother behavior as a function of L , and it may indeed be more accurate to use the alternative definition⁷ of the strong-absorption radius in terms of the half-way point of the function $1 - |\eta_L|^2$. Typical cross sections given by these potentials are shown in Figs. 4-7.

A comparison of results for the strong-absorption radii is given in Table V. For the purposes of this

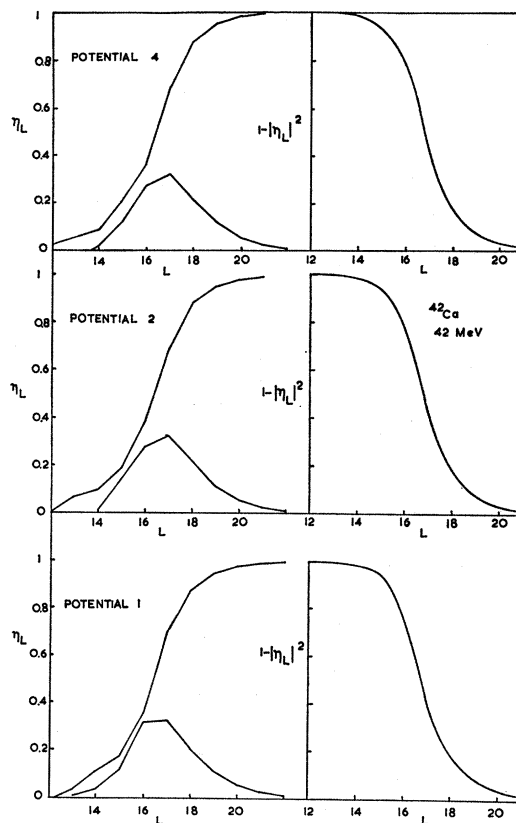


FIG. 1. The real and imaginary parts of the reflection coefficients η_L and the absorption coefficients $1 - |\eta_L|^2$ given by potentials which fit the data on ^{42}Ca at 42 MeV. The parameters of the potentials are given in Table II.

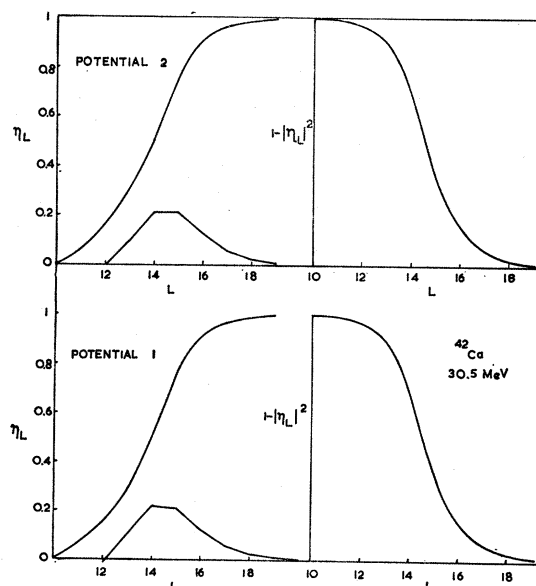


FIG. 2. The real and imaginary parts of the reflection coefficients η_L and the absorption coefficients $1 - |\eta_L|^2$ given by potentials which fit the forward-angle data on ^{42}Ca at 30.5 MeV. The parameters of the potentials are given in Table III.

¹⁷ C. G. Morgan, Rutherford High Energy Laboratory PLA Report, 1966 (unpublished); and (to be published).

¹⁸ R. J. Peterson, Ph.D. thesis, University of Washington, 1966 (unpublished).

¹⁹ C. Gruhn and N. S. Wall, Nucl. Phys. **81**, 161 (1966).

²⁰ G. Bruge, Saclay Report No. CEA-R3147, 1967 (unpublished).

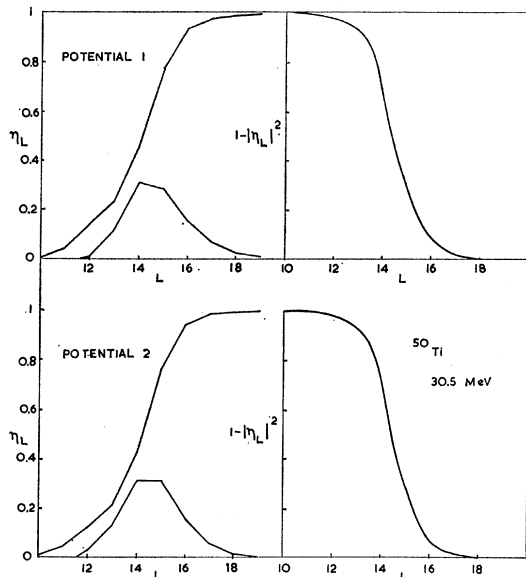


FIG. 3. As in Fig. 2, but for ^{50}Ti .

comparison it must be noted that the formulas given by Eqs. (4a) and (4b) describe the general trend for a wide range of nuclei but individual nuclei are known

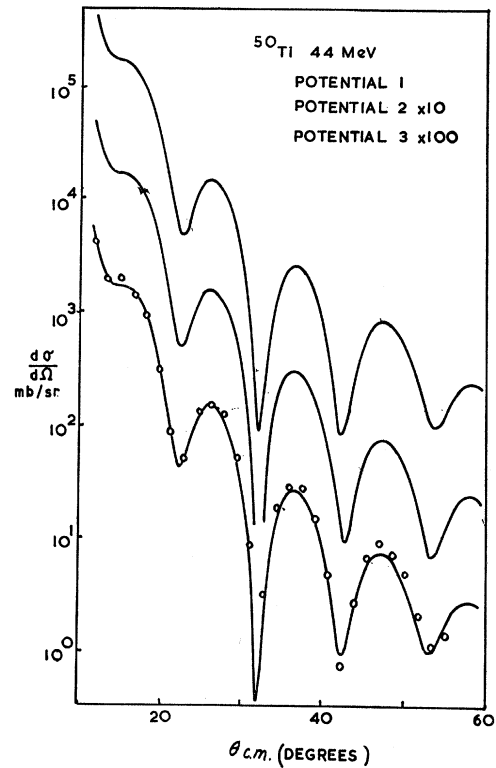


FIG. 5. Cross sections for elastic scattering from ^{50}Ti at 44 MeV obtained from some of the potentials given in Table IV. The data is that of the Saclay group (Ref. 20).

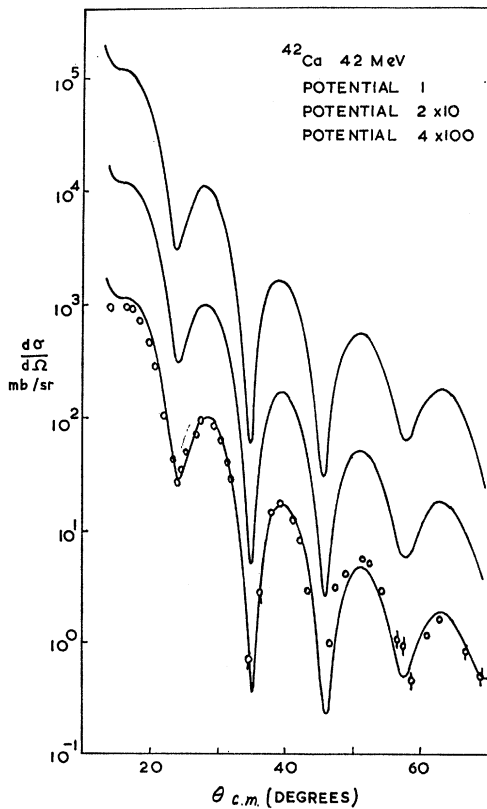


FIG. 4. Cross sections for elastic scattering for ^{42}Ca at 42 MeV obtained from some of the potentials given in Table II. The data is that of Peterson (Ref. 18).

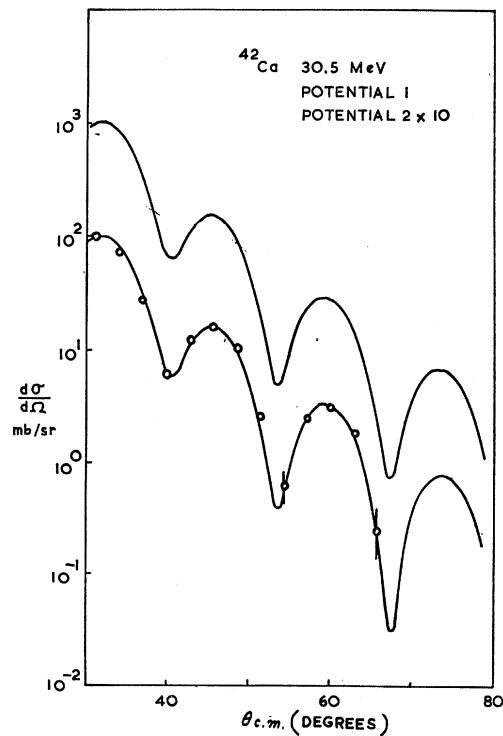


FIG. 6. Cross sections for elastic scattering from ^{42}Ca at 30.5 MeV obtained from the potentials given in Table III. The data is that of Gruhn and Wall (Ref. 19).

to show deviations from this trend, and that the analysis of Blair and Fernandez has been carried out with much more accurate data than has hitherto been available. In these circumstances the agreement between the results for ^{42}Ca at 42 MeV seems quite satisfactory, and so is the agreement for ^{50}Ti . There is some discrepancy between the results obtained at 30.5 MeV and 42–44 MeV which might suggest some energy dependence²¹ for the strong-absorption radius, but the lower-energy data are notoriously difficult to fit^{16,19} and we have fitted only a restricted angular range at 30.5 MeV.

We have also investigated the behavior of the optical-model wave function. This is given by the usual formula

$$\psi = \sum_L i^L (2L+1) f_L(kr) P_L(\cos\theta),$$

where $f_L(kr)$ is the solution of the radial Schrödinger equation and θ is the angle of scattering. By evaluating $|\psi|$ as a function of r for $\theta=0$ and $\theta=180$ we obtain a picture of the variation of the modulus of the wave function along the z axis, which is taken in the normal way to be along the direction of the incident beam. Results for various potentials are shown in Figs. 8 and

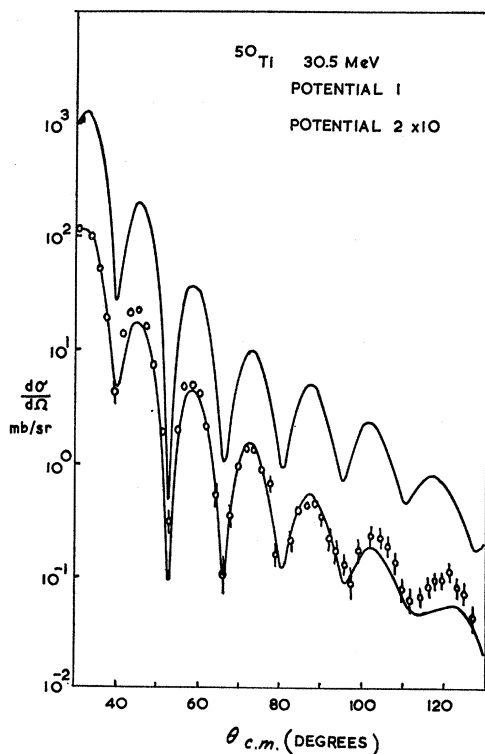


FIG. 7. As in Fig. 6, but for ^{50}Ti .

²¹ The possibility that such energy dependence should occur is discussed by Blair (Ref. 3) and by E. Rost and N. Austern, Phys. Rev. 120, 1375 (1960).

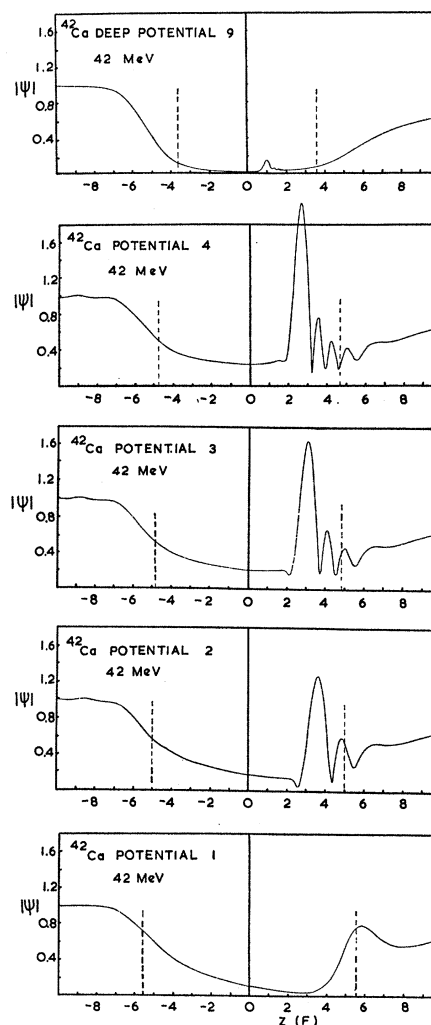


FIG. 8. The moduli of the optical-model wave functions for scattering from ^{42}Ca at 42 MeV obtained from some of the potentials given in Table II. The wave functions are calculated along the z axis with the origin at the center of the potential, and the dotted lines indicate the position of the half-way radius of the potential.

9. From these results it can be seen that on the illuminated side of the nucleus, (i.e., $z < 0$), the moduli of the wave functions given by equivalent potentials show very similar behavior, and in particular that the absorption effect on the wave function begins in the vicinity of the strong-absorption radius. Thus we see that the strong-absorption radius has a very real physical significance as a measure of the distance from the origin at which the process of absorption begins to be effective. Using the definition of the strong-absorption radius as the turning point for the critical angular momentum L_0 , we conclude that the condition that the real parts of the potentials are identical ensures that the partial waves around L_0 have the same reflection coefficients.

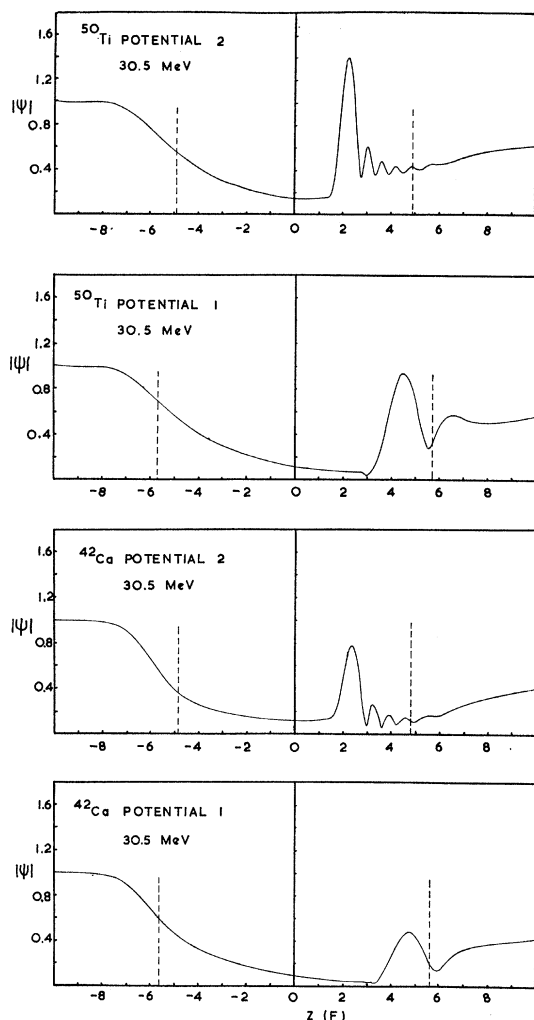


FIG. 9. The moduli of the optical-model wave functions for scattering from ^{42}Ca and ^{60}Ti at 30.5 MeV obtained from the potentials given in Table III. The wave functions are calculated along the z axis with the origin at the center of the potential, and the dotted lines indicate the position of the half-way radius of the potential.

The discussion given above of the significance of the strong-absorption radius is entirely in the spirit of the original use of this parameter in the Fraunhofer-diffraction model.³ However, we know that this model is incomplete, and the other effects of the potential, particularly in the interior region, can be seen from the behavior of $|\psi|$ on the dark side of the nucleus, where

the now familiar focus^{11,22} is formed. As the strength of the real part of the potential is increased the focusing effect becomes stronger, i.e., the focus increases in intensity and moves farther inside the nucleus. At the same time, secondary peaks are formed because of interference of the incident beam with a beam reflected from the far surface of the nucleus. For the very deep potential (potential 9 of Table II) the focus moves still farther inside the nucleus, but in this case the imaginary part of the potential is so large that the intensity on the dark side of the nucleus is drastically reduced. Only in this latter case can it be said that the probability for the α particle to penetrate into the interior of the nucleus is negligibly small. The behavior of the wave functions on the dark side of the nucleus does not indicate any special role for the strong-absorption radius in this region.

4. CONCLUSIONS

From our study of groups of optical-model potentials which fit the data on the elastic scattering of medium-energy α particles we have obtained the following answers to the questions posed in the Introduction.

(1) The Igo criterion in the form of Eq. (7) is valid only if very little variation is allowed in the diffuseness parameter a .

(2) An alternative criterion of wider applicability is obtained from the requirement that the real parts of the potentials should be equal at the strong-absorption radius, and that the imaginary parts should be small and approximately equal at this radius.

(3) Because of the ambiguities possible for strongly absorbed projectiles, the half-way radius and the equivalent radius of the real potentials are functions of the depth of the potential and therefore cannot be regarded as significant size parameters. The strong-absorption radius, however, appears to be a very significant size parameter. Again, because of the ambiguities, this parameter cannot usefully be related to the potential parameters, and its interpretation in terms of nuclear size parameters requires a microscopic description of elastic scattering.⁹

ACKNOWLEDGMENTS

We gratefully acknowledge valuable correspondence and encouragement from Professor J. S. Blair.

²² I. E. McCarthy, Nucl. Phys. **10**, 583 (1959); **11**, 574 (1959); Phys. Rev. **128**, 1237 (1962).